



Peer review status:

This is a non-peer-reviewed preprint submitted to EarthArXiv.

Dynamic Line Rating and Residual Congestion: Implications for Storage Sizing and Availability

Prashant Pant*, Thomas Hamacher*, Reinaldo Tonkoski Jr.*

*Technical University of Munich (TUM), Munich, Germany

Email: {prashant.pant, thomas.hamacher, reinaldo.tonkoski}@tum.de

Abstract—Dynamic line rating (DLR) can recover transfer capacity on wind dominated corridors because high wind generation often coincides with stronger conductor cooling. This paper examines a 380 kV Schleswig-Holstein export corridor and compares five operating cases: a static baseline, conservative DLR, two DLR paired battery energy storage system (BESS) configurations sized to the 95th and 99.5th percentile of residual overload, and a standalone BESS without DLR. A full year deterministic simulation using IEEE 738-2012 thermal modelling and ERA5 weather data shows that conservative DLR alone reduces annual curtailment by 95.8%, from 87 177 to 3 689 MWh, with payback below one year. Adding a small DLR paired BESS at the 95th percentile sizing point (21 MW/70 MW h) increases the total curtailment reduction to 97.7%, while the 99.5th percentile variant (22 MW/72 MW h) yields almost no further benefit. A standalone BESS sized to the same percentile rule (173 MW/254 MW h) achieves only 26.2% reduction because its rated discharge window is too short for the multi hour and multi day winter congestion that dominates this corridor. DLR therefore does more than lift the transfer limit. It also changes the shape of the remaining congestion, which sharply reduces the storage size needed for residual relief.

Index Terms—dynamic line rating, battery energy storage, wind curtailment, IEEE 738, congestion management, transmission planning

I. INTRODUCTION

Wind curtailment due to transmission congestion is a growing operational and economic challenge. In Germany, approximately 19 TW h of renewable generation was curtailed in 2023 at a redispatch cost of €3.1 billion, with the majority concentrated on north-to-south corridors from wind-rich coastal states [1]. Schleswig-Holstein alone hosts over 9 GW of onshore wind capacity, generating roughly 150% of local demand, yet transmission to southern load centres remains capacity-constrained pending completion of major HVDC links after 2027 [2].

Dynamic line rating offers a near-term, low-capital solution. By computing real-time conductor ampacity from the IEEE 738 or CIGRE heat balance equations using weather measurements or forecasts, DLR captures the natural correlation between high wind speeds and increased conductor cooling [3], [4]. Field deployments consistently report 10–40% average capacity gains over static ratings [5], and regulatory momentum is accelerating: FERC Order 881 mandates ambient-adjusted ratings for U.S. transmission by July 2025 [6], while European TSOs increasingly adopt DLR as a grid-enhancing technology for congestion management [7].

Battery energy storage (BESS) is frequently proposed as a complementary or alternative measure for congestion relief [8], [9]. Several studies address joint DLR-BESS operation [10], [11], and recent work combines DLR with BESS and optimal transmission switching in unit commitment frameworks [12]. However, existing studies typically evaluate DLR and BESS as a combined hybrid system without isolating the individual contribution of each technology, quantifying how the presence of DLR changes the BESS sizing requirement, or analysing the failure modes of standalone BESS against structurally persistent congestion.

This paper examines a single 380 kV wind export corridor over a full calendar year at 15 minute resolution and isolates the separate roles of DLR and storage through five scenarios. The paper makes three contributions:

- 1) It quantifies how much curtailment reduction comes from DLR alone (95.8%) and how little remains for storage to address once the transfer limit is weather adjusted.
- 2) It explains why standalone BESS performs poorly on this corridor. Congestion during major winter wind events persists for hours to days, while the battery discharge window at rated power is only 1.4 hours.
- 3) It shows that DLR changes the residual congestion structure enough to reduce the storage requirement sharply. After DLR, a 21 MW/70 MW h BESS captures almost all remaining value, while tightening the sizing percentile to 99.5 offers negligible additional benefit.

The analysis uses reanalysis weather data and a simplified loading model. It does not include network power flow, N-1 security constraints, or explicit stochastic forecast modelling. These limitations are discussed in Section VI.

II. RELATED WORK

DLR is well established as a means of increasing usable transfer capacity when ambient conditions are favourable. Karimi et al. survey thermal rating methods and field deployments, while Peña-Asensio et al. review recent DLR technologies and applications [3], [4]. For northern German corridors, Glaum and Hofmann report strong DLR potential on wind dominated export lines, although practical gains are reduced by forecasting uncertainty, weakest span effects, and equipment limits [2]. These studies support the case for DLR, but they do not answer how much residual congestion remains once conservative operating margins are applied.

BESS has also been studied as a congestion relief measure. Lindner et al. show that storage can reduce redispatch on the German transmission grid, but they also note that storage alone is difficult to justify economically for this role [9]. Song et al. and Nour et al. address storage sizing for transmission level renewable integration and curtailment reduction [8], [13]. That literature is useful for battery sizing, but it does not explain how the role of storage changes once DLR has already removed most of the overload.

A smaller body of work studies DLR and storage jointly. Dehghani-Sanij et al. consider chance constrained scheduling of DLR and BESS, Mateo et al. compare them as non wire alternatives, and Teh et al. combine DLR, storage, and transmission flexibility in operational frameworks [10]–[12]. The gap addressed here is narrower and practical: for a wind correlated export corridor, how much value comes from DLR alone, how much storage remains justified afterward, and why does standalone storage fail when congestion is persistent rather than spiky?

III. CORRIDOR AND THERMAL MODEL

A. Conductor and static rating

The study conductor is Al/St 380/50 ($D = 26.8$ mm, $R_{DC,20} = 76.2 \mu\Omega \text{ m}^{-1}$) on a 380 kV Schleswig-Holstein north-to-south corridor. The steady-state IEEE 738-2012 heat balance [14] under a conservative reference state ($T_a = 35^\circ\text{C}$, $V_w = 0.6 \text{ m s}^{-1}$, $Q_s = 900 \text{ W m}^{-2}$, $T_{\max} = 80^\circ\text{C}$), consistent with German TSO practice [2], yields:

$$S_{\text{static}} = \sqrt{3} U I_{\text{static}} = 511.6 \text{ MV A}. \quad (1)$$

B. DLR computation and derating chain

The real-time ampacity at interval k solves the steady-state heat balance:

$$I_{\text{DLR},k} = \sqrt{\frac{Q_{c,k} + Q_{r,k} - Q_{s,k}}{R_{ac}(T_{\max})}}, \quad (2)$$

where Q_c , Q_r , Q_s denote convective cooling, radiative cooling, and solar heat gain per unit length [14]. Meteorological inputs for 2023 are taken from ERA5 reanalysis at Brunsbüttel (53.89°N , 9.13°E), resampled to 15-minute intervals, as a proxy for corridor sensor readings.

The raw IEEE 738 ampacity is converted to an operator-usable limit through a derating chain (Fig. 1) reflecting established practice. Each factor addresses a distinct source of uncertainty or operational constraint:

- 1) *Hourly averaging* ($k_h = 0.95$): accounts for sub-hourly wind variability within a dispatch interval [2].
- 2) *Span aggregation and wind angle* ($k_{\text{span}} = 0.74$): the corridor rating is governed by the weakest span; spatial wind speed and attack-angle variability reduce the effective ampacity below the point measurement [4].
- 3) *Forecast uncertainty* ($k_f = 0.84$): day-ahead DLR forecast errors of 8–15% are reported in the literature [12], [15]; a 2σ margin at the conservative (8%) end gives $k_f = 1 - 2.05 \times 0.08 \approx 0.84$.

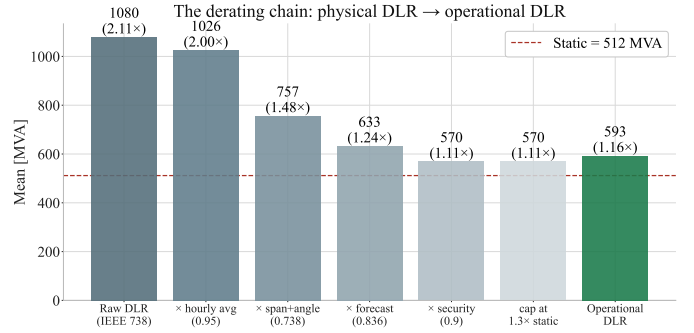


Fig. 1. Derating chain from raw IEEE 738 DLR to operative limit. Each bar shows the mean DLR after applying the cumulative derating factors. The dashed line is the static rating.

- 4) *TSO safety margin* ($\alpha = 0.90$): a 10% coordination margin adopted from Elia/CORESO practice [5].
- 5) *Equipment cap* ($\gamma = 1.30$): the practical rating ceiling of corridor switchgear and transformers, limiting the operative DLR to 130% of static [5].

The composite derating on uncapped DLR is $k_h \times k_{\text{span}} \times k_f \times \alpha \approx 0.53$. The operative limit at interval k is then:

$$S_k^{\text{lim}} = \max\left(S_{\text{static}}, \min\left(S_k^{\text{raw}} \cdot 0.53, \gamma S_{\text{static}}\right)\right). \quad (3)$$

The maximum operative limit is $\gamma S_{\text{static}} = 665.1 \text{ MV A}$ (30% above static). The resulting annual mean operative DLR is 593 MV A (1.16x static), consistent with the 10–17% usable DLR gain reported by European TSOs after applying operational constraints [2], [5].

Figure 2 shows the operative DLR during the highest-congestion two-week period, illustrating how the derating chain filters the raw thermal potential. The raw DLR frequently exceeds 2x static, but only ~16% of the thermal physics translates into usable headroom after operational derating.

C. Corridor loading

Corridor loading is proxied as an IEC-standard wind power curve (1500 MW installed, hub height 100 m) at 40% corridor participation, plus a diurnally and seasonally modulated base transit flow (mean 60 MW). The resulting mean corridor flow is 151 MW (29% of static), with a peak of 687 MW (134% of static). The wind generation achieves a capacity factor of 15.1%. Congestion occurs exclusively during high-wind events when generation peaks exceed the transfer limit, a pattern common to northern German export corridors [2]. Over the simulated year, 419 distinct congestion events occur under the static rating (S0), with a median event duration of 0.5 hours and a 95th-percentile duration of 8 hours. Two events exceed 24 hours. Winter months (December–February) contribute 54.6% of total annual curtailment, with December alone accounting for 23.2%.

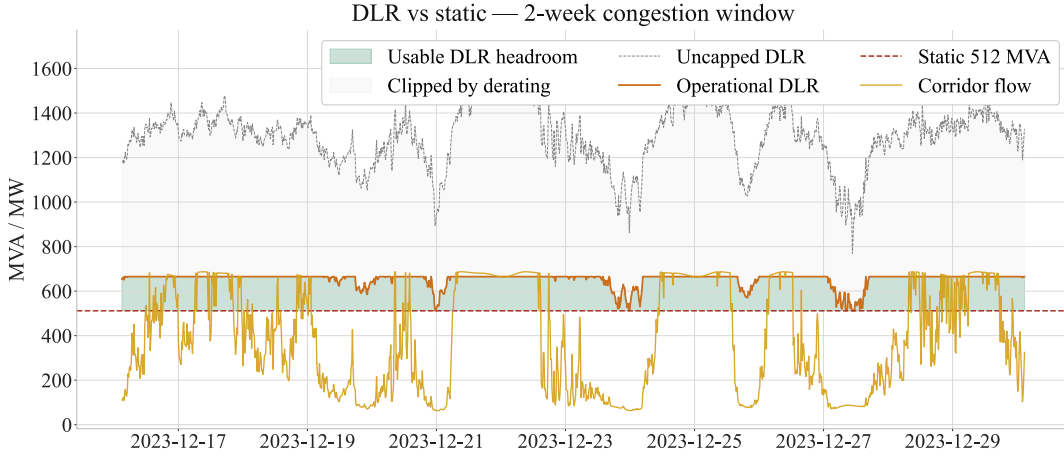


Fig. 2. Two-week congestion window showing corridor flow (gold), static limit (red dashed), operative DLR after full derating (orange), and raw IEEE 738 ampacity (grey dashed). The green fill indicates usable DLR headroom; the grey fill shows capacity filtered by the derating chain.

TABLE I
SIMULATION SCENARIOS

| ID | Name | Description |
|----|---------------|---|
| S0 | Static | Static limit only. Reference. |
| S1 | DLR-cons | Operative DLR per Eq. (3). No BESS. |
| S2 | DLR+BESS-95 | DLR-cons + BESS sized at 95th-pct. |
| S4 | DLR+BESS-99.5 | DLR-cons + BESS sized at 99.5th-pct. |
| S3 | BESS-only | Static limit + standalone BESS. No DLR. |

IV. METHODOLOGY

A. Scenario definition

Five scenarios are evaluated by replaying the full 2023 calendar year at 15-minute resolution (35 011 intervals). Table I lists the scenario definitions.

At each interval, the effective transfer limit is computed from weather inputs. Curtailment is $C_k = \max(F_k - S_k^{\text{eff}}, 0)$ where F_k is the total corridor flow and S_k^{eff} is the applicable limit (including any BESS discharge contribution).

B. BESS sizing

BESS power for each scenario is sized to the p th percentile of non-zero residual curtailment under the corresponding transfer limit, following the percentile-based approach of [13]. For S2 and S4, the residual is computed against the DLR limit (S1 residual); for S3, against the static limit (S0 residual). Energy capacity uses a 30-minute redispatch window adjusted for round-trip efficiency:

$$E = \frac{P \cdot \tau}{\eta_{RT}}, \quad (4)$$

with $\tau = 0.5$ h and $\eta_{RT} = 0.92$.

Applying the 95th-percentile rule (S2) yields 21.2 MW/70.2 MW h. Tightening to the 99.5th percentile (S4)

increases the sizing only marginally to 21.8 MW/72.4 MW h, because the DLR-reduced residual overload distribution has a heavy lower tail and a very compressed upper tail. The standalone BESS (S3), sized to the 95th percentile of S0 overload, requires 173.3 MW/254.3 MW h.

C. BESS dispatch

Dispatch follows a rolling-horizon linear programme (LP) over 24-hour blocks that minimises total residual curtailment subject to SOC tracking:

$$\text{SOC}_{k+1} = \text{SOC}_k - \frac{P_{\text{dis},k}}{\eta_{\text{dis}}} \Delta t + P_{\text{chg},k} \eta_{\text{chg}} \Delta t, \quad (5)$$

with $\eta_{\text{ch}} = \eta_{\text{dis}} = \sqrt{0.92}$, $\Delta t = 0.25$ h, and bounds $\text{SOC} \in [0.10E, E]$. Initial SOC is set to 50% of capacity. When the LP is infeasible (rare), a greedy fallback discharges to suppress overflows and recharges from spare headroom. The LP formulation ensures that the battery is used optimally within each 24-hour lookahead, avoiding myopic depletion that would leave capacity unavailable for subsequent events within the same block.

D. Indicative economics

Simple payback is computed as $t_{pb} = \text{CapEx} / V$, where V is the annual curtailment saving valued at €65/MWh and CapEx uses €280 k/MWh for BESS and €0.6M for DLR installation [5], [16]. The €65/MWh curtailment cost reflects average German wholesale prices plus EEG compensation. These are indicative estimates; a full economic assessment would require degradation modelling, opportunity costs, and revenue stacking.

V. RESULTS

A. Annual curtailment

Table II summarises the annual results and Figs. 3–8 show the main patterns.

Three findings are central.

TABLE II
ANNUAL SIMULATION RESULTS (ERA5 2023, IEEE 738-2012)

| Scenario | Curt. [MWh] | Red. [%] | BESS [MW] | CapEx [M€] | PB [yr] |
|-------------------|-------------|----------|-----------|------------|---------|
| S0: Static | 87 177 | – | – | – | – |
| S1: DLR-cons | 3 689 | 95.8 | – | 0.6 | 0.1 |
| S2: DLR+BESS-95 | 2 004 | 97.7 | 21.2 | 20.3 | 3.7 |
| S4: DLR+BESS-99.5 | 1 976 | 97.7 | 21.8 | 20.9 | 3.8 |
| S3: BESS-only | 64 312 | 26.2 | 173.3 | 71.2 | 47.9 |

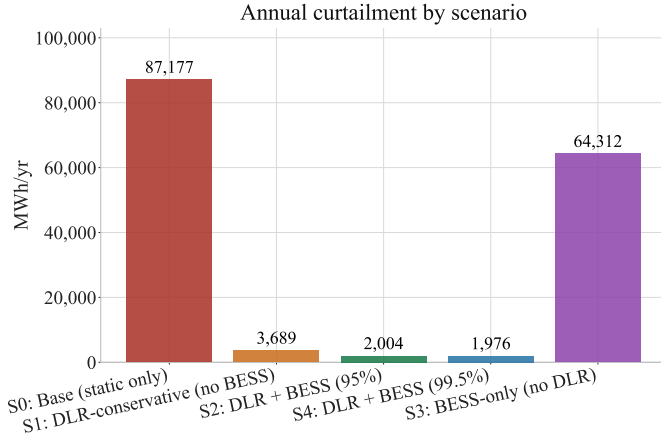


Fig. 3. Annual curtailment by scenario. DLR alone captures most of the available reduction. Adding storage after DLR yields only a modest further gain, while standalone BESS remains ineffective for the dominant winter overload.

First, DLR is the dominant intervention on this corridor. Scenario S1 reduces curtailment by 95.8% with very low capital cost. That result follows from the corridor physics: the same weather that drives export peaks also cools the conductor, so high wind periods are also the periods with the largest rating uplift. Congested hours fall from 651 in S0 to 322 in S1, and the remaining events are shallower and shorter.

Second, adding storage after DLR offers only limited incremental value. S2 raises the total reduction from 95.8% to 97.7%. Moving from the 95th percentile sizing to the 99.5th percentile adds only 2.2 MWh of storage and saves 28 MWh/year of extra curtailment. For this reason, S2 is the practical sizing point and S4 mainly serves to show how quickly diminishing returns set in.

Third, standalone storage is a poor substitute for DLR on this corridor. S3 uses far more installed power and energy than S2, yet it achieves only 26.2% curtailment reduction. The reason is not dispatch quality or insufficient power rating. It is the duration and clustering of winter congestion, which repeatedly deplete the battery before the event is over.

B. Monthly profile

Figure 4 shows the monthly curtailment breakdown. Congestion is concentrated in winter, especially from November to March, when North Sea weather systems produce sustained wind output. December is the largest single month in S0



Fig. 4. Monthly curtailment. Winter months dominate congestion volume (54.6% from December–February alone); the scenario ranking is stable across all months. The standalone BESS (S3) tracks S0 closely in winter, confirming the structural congestion argument.

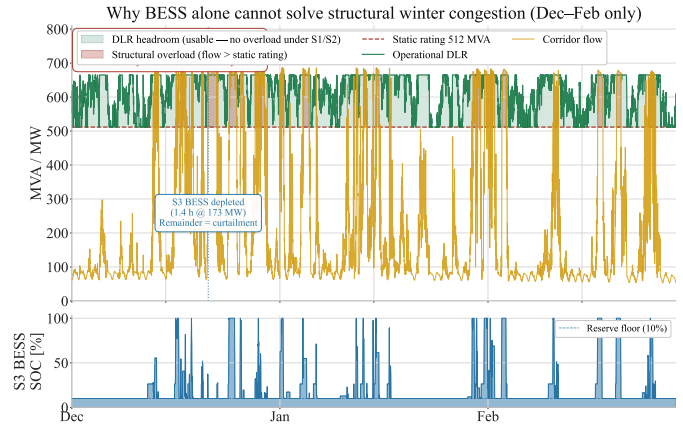


Fig. 5. Winter congestion analysis (December–February). Top panel: corridor flow (gold), static rating (red dashed), and operative DLR (green). Red shading marks overload above the static limit, while green shading shows usable DLR headroom. The blue dotted line marks the point where the S3 battery (254 MWh/173 MW) is exhausted at rated discharge. Bottom panel: S3 battery SOC during the same period, showing repeated depletion.

with 20,219 MWh, followed by January and February. The scenario ranking is stable across the winter season. S1 remains close to zero relative to S0 in every high congestion month, while S3 tracks S0 much more closely. This reinforces the central point: on this corridor, DLR addresses the dominant congestion directly, whereas standalone storage struggles when overload persists for several hours or recurs before recharge is complete.

C. Why standalone BESS cannot resolve structural congestion

Figure 5 provides the key evidence for the S3 result. The top panel shows corridor flow against the static and DLR limits through December to February, with long continuous overload runs marked explicitly. The bottom panel shows the S3 state of charge over the same period.

The problem is structural rather than marginal. Winter overload energy above the static limit totals 47,626 MWh in December to February alone. The S3 battery stores 254.3 MWh,

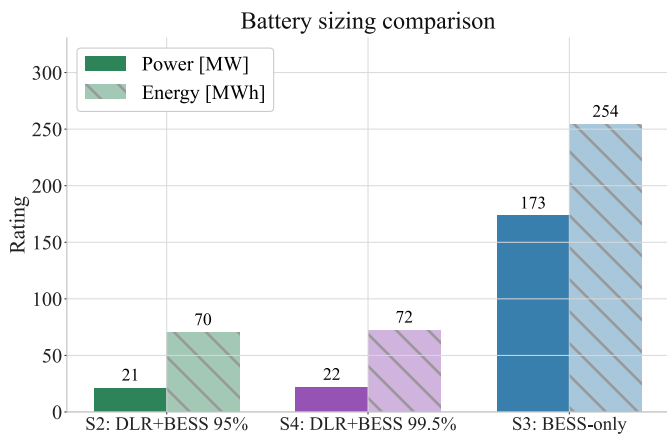


Fig. 6. Battery sizing comparison across the three storage configurations. DLR reduces the storage requirement sharply, while the 99.5th percentile case adds very little over S2.

which is about 0.5% of that winter volume. Even across the full year, the overload energy is 343 times the battery energy capacity. A percentile based battery sized for peak shaving is therefore poorly matched to congestion that persists over long weather events.

Duration matters as much as energy. At rated power, the S3 battery depletes in about 1.4 hours. The median event is shorter than this, but the events that dominate total curtailment are in the long tail. The 95th percentile event lasts 8 hours and the two longest events exceed 24 hours. Once a major event begins, the battery can only cover the first part of the overload.

The state of charge trace shows the operational consequence. The battery repeatedly falls to or near its reserve floor during winter. Across all 419 annual congestion events, average event start SOC is only 43%, and 139 events begin below 15% SOC. So even when installed power is available on paper, usable discharge capability is often absent when the next event arrives.

DLR changes this picture before storage is used. When DLR raises the transfer limit, most of the overload disappears directly and the residual events are smaller. That leaves room for a much smaller battery to remain available across successive peaks.

D. BESS sizing and the SOC recharge mechanism

Figure 6 compares the three storage configurations. With DLR in place, the required BESS size drops from 173.3 MW/254.3 MWh in S3 to 21.2 MW/70.2 MWh in S2. That corresponds to a 72% reduction in energy capacity and an 88% reduction in power. Moving to the 99.5th percentile adds only 2.2 MWh.

This reduction is not only a matter of lower residual volume. It also reflects different state of charge dynamics. In S3, the battery works against a fixed static limit, so once a major event begins it discharges early and then remains near empty while later peaks arrive. In S2, DLR absorbs most of the overload directly and leaves intervals of headroom between

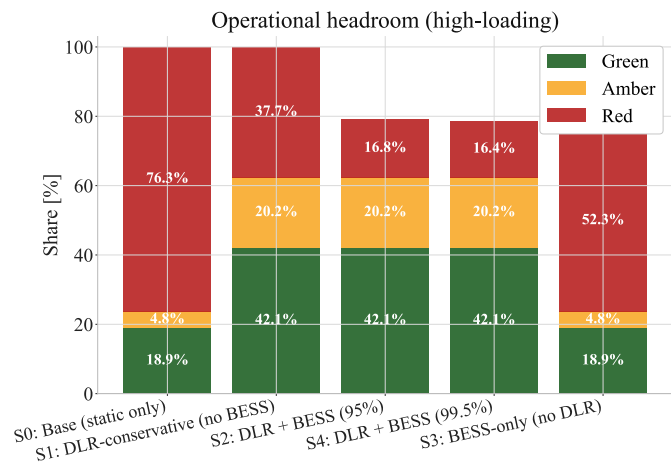


Fig. 7. Operational headroom during high loading intervals (>80% of static capacity). Even with much less installed energy, S2 shows fewer fully congested intervals than S3 because DLR leaves recharge opportunities between peaks.

TABLE III
BESS DISPATCH SUMMARY

| Metric | S2 | S4 | S3 | S3/S2 |
|----------------------|------|------|-------|-------|
| Power [MW] | 21.2 | 21.8 | 173.3 | 8.2× |
| Energy [MWh] | 70.2 | 72.4 | 254.3 | 3.6× |
| Ann. discharge [MWh] | 1685 | 1712 | 22865 | 13.6× |
| Equiv. full cycles | 24 | 24 | 90 | 3.8× |
| CapEx [M€] | 20.3 | 20.9 | 71.2 | 3.5× |
| Payback [yr] | 3.7 | 3.8 | 47.9 | 12.9× |

peaks even during active weather systems. That headroom allows the battery to recharge and stay available for the remaining residual overload.

Figure 7 shows the same effect through a simple headroom classification during high loading intervals. Despite its much smaller energy capacity, S2 produces fewer fully congested intervals than S3. S2 and S4 also look almost identical, which is consistent with the very small sizing difference between them.

Table III summarises dispatch statistics. The DLR paired batteries act as low duty residual relief assets, while the standalone battery behaves like a high throughput bulk storage plant. That difference matters not only for capital cost but also for degradation and replacement economics.

E. Cumulative curtailment and seasonal patterns

Figure 8 presents the cumulative curtailment trajectories for all five scenarios. The staircase structure of S0 and S3 reveals that curtailment accumulates in discrete winter storm clusters rather than continuously, with the steepest segments in December, January, and February. S1, S2, and S4 track near-zero throughout, confirming DLR effectiveness across all congestion periods. S3 tracks S0 closely for the largest steps, visually confirming that the standalone BESS cannot absorb

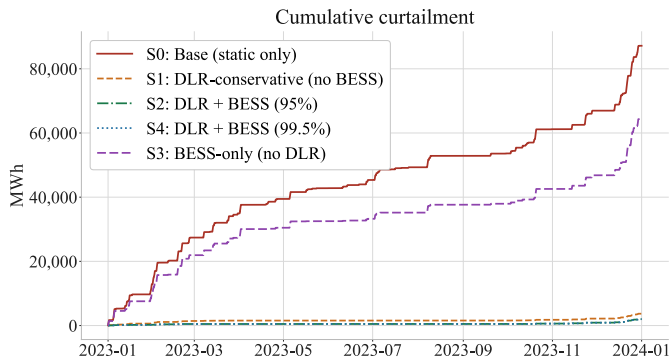


Fig. 8. Cumulative curtailment for all five scenarios. The step-like structure of S0 and S3 corresponds to winter storm clusters. S3 (BESS-only) tracks S0 closely during the largest steps, confirming that the standalone battery cannot absorb the structural overload that dominates annual curtailment.

the structural winter overload that constitutes the majority of annual curtailment.

VI. DISCUSSION

A. Interpretation and generalisability

The main result, 95.8% curtailment reduction from DLR alone, is tied to the corridor type studied here. Average loading is modest, and congestion appears mainly during high wind export periods that also provide the strongest conductor cooling. This is exactly the setting in which DLR is most effective.

The result should not be extended mechanically to every corridor. Where congestion is driven by summer demand peaks, weak wind conditions, or broader network constraints, the benefit of DLR will be lower and the relative role of storage may be larger. The quantitative values reported here are corridor specific, but the qualitative message is more general for wind correlated export corridors: DLR removes most of the problem first, then storage can be sized for the smaller residual.

The standalone BESS result also needs proper framing. A larger battery could reduce more curtailment, but the required energy capacity would move toward the scale of the persistent overload itself. For this type of corridor, the issue is not dispatch quality. It is a mismatch between long duration congestion and practical battery energy capacity.

B. Limitations

Several modelling simplifications bound the quantitative conclusions. A single ERA5 grid point is used as a proxy for corridor weather. Actual operative rating depends on the weakest span, and within corridor variability can reduce usable DLR relative to a point estimate [4]. That effect is partly represented through the span aggregation factor, but direct span measurements would improve accuracy.

The loading model is intentionally simple. It captures wind driven export behaviour but not network power flow, redispatch interactions, or N-1 security constraints. A full AC optimal power flow model would likely reduce the absolute headroom

values, although the comparative ranking between scenarios is less likely to change.

Only one weather year is simulated. Different wind years would shift the absolute curtailment totals. Forecast uncertainty is represented conservatively through the derating chain, but not as an explicit stochastic process. Battery degradation, opportunity cost, and stacked revenue streams are also outside scope, so the economics should be read as indicative rather than bankable.

C. Practical implications

For TSOs and regulators assessing congestion relief on wind export corridors, the sequence is straightforward. First, deploy DLR as the low capital intervention that captures most of the available benefit. Second, if residual curtailment remains material, size storage against the DLR reduced residual rather than the original static overload. On this corridor, that changes the storage requirement dramatically and avoids the capital inefficiency of deploying standalone BESS too early.

The results also suggest that attention should shift from raw conductor physics to implementation constraints. Forecast quality, weakest span representation, and equipment limits will often determine how much of the thermal potential becomes usable in practice. These issues are likely to matter more for real deployment than small refinements in battery sizing percentile beyond the 95th percentile.

VII. CONCLUSION

This paper compared DLR and storage on a wind dominated 380 kV export corridor and separated what each technology contributes to curtailment reduction.

Conservative DLR alone reduces annual curtailment by 95.8% with payback below one year. Adding a DLR paired BESS sized to the 95th percentile residual (21 MW/70 MW h) raises the total reduction to 97.7%. Increasing the sizing percentile to 99.5 changes the result only marginally, which shows that the 95th percentile already captures the practical sizing point.

A standalone BESS sized by the same percentile rule performs much worse, achieving only 26.2% reduction. The reason is that the dominant congestion on this corridor is persistent winter overload, not isolated short spikes. Those events exhaust the battery quickly and recur before recharge is restored.

The main implication is that DLR does not only increase transfer capacity. It changes the temporal structure of the residual congestion that storage must handle. For wind correlated export corridors, that makes DLR the primary intervention and leaves storage with a narrower but still useful role as a residual relief asset.

Future work should test the same logic in a full network model with security constraints, stochastic DLR forecasts, multi year weather ensembles, and battery degradation.

REFERENCES

- [1] Bundesnetzagentur, "Congestion Management Reports — SMARD Transparency Platform," 2024. [Online]. Available: <https://www.smard.de/page/en/topic-article/5892/215186>
- [2] P. Glaum and L. Hofmann, "Assessing the benefits of dynamic line rating for redispatch reduction in the German transmission grid," *Electric Power Systems Research*, vol. 220, p. 109301, 2023.
- [3] S. Karimi, P. Musilek, and A. M. Knight, "Dynamic thermal rating of transmission lines: A review," *Renewable and Sustainable Energy Reviews*, vol. 91, pp. 600–612, 2018.
- [4] A. Peña-Asensio, B. Arnedo-García, D. Treballe, and C. Gallego-Castillo, "Dynamic line rating: A review of technologies and applications," *Renewable and Sustainable Energy Reviews*, vol. 189, p. 114028, 2024.
- [5] International Renewable Energy Agency, "Innovation Landscape Brief: Dynamic Line Rating," IRENA, Abu Dhabi, Tech. Rep., 2020. [Online]. Available: <https://www.irena.org/publications/2020/Feb/Dynamic-line-rating>
- [6] Federal Energy Regulatory Commission, "Order No. 881 — Managing Transmission Line Ratings," Dec. 2021, docket No. RM20-16-000. [Online]. Available: <https://www.ferc.gov/media/order-no-881>
- [7] I. Itodo, L. Mehigan, P. Deane, and A. Foley, "Dynamic line rating for transmission systems: a review of operational integration and future directions," *IET Generation, Transmission & Distribution*, vol. 19, no. 1, p. e13082, 2025.
- [8] Y. Song, Q. Wu, H. Zhao, and M. Zhang, "Battery energy storage sizing for enhancing renewable hosting capacity at transmission level," *IEEE Transactions on Power Delivery*, vol. 39, no. 2, pp. 1021–1033, 2024.
- [9] M. Lindner, T. Hess, F. Scheidt, and T. Leibfried, "Operation strategies of battery energy storage systems for preventive and curative congestion management in transmission grids," *IET Generation, Transmission & Distribution*, vol. 17, no. 7, pp. 1528–1541, 2023.
- [10] M. Dehghani-Sanij, M. Fotuhi-Firuzabad, and F. Aminifar, "Chance-constrained operation of battery storage under dynamic line rating forecast uncertainty," *Electric Power Systems Research*, vol. 228, p. 109987, 2024.
- [11] C. Mateo, R. Cossent, T. Gómez, and L. Olmos, "Non-wire alternatives for transmission congestion: Dynamic line rating versus battery storage in wind-rich networks," *Applied Energy*, vol. 357, p. 122487, 2024.
- [12] J. Teh and Z. N. Zainuddin, "Probabilistic dynamic line rating assessment for wind-integrated transmission systems," *IEEE Transactions on Power Delivery*, vol. 38, no. 4, pp. 2891–2901, 2023.
- [13] M. Nour, J. P. Chaves-Ávila, P. García-Triviño, and R. Catalán-Ros, "Optimal sizing of battery energy storage for curtailment reduction in heavily loaded transmission corridors," *IEEE Transactions on Smart Grid*, vol. 15, no. 2, pp. 1876–1889, 2024.
- [14] IEEE, "IEEE Standard for Calculating the Current-Temperature Relationship of Bare Overhead Conductors," IEEE Std 738-2012, 2013.
- [15] M. Bakhtvar and A. Keane, "Probabilistic dynamic line rating for wind-heavy transmission corridors: Forecast uncertainty and operational confidence bounds," *IEEE Transactions on Sustainable Energy*, vol. 15, no. 1, pp. 312–323, 2024.
- [16] P. Simshauser, "Transmission investment in renewable energy zones: The role of dynamic line rating," *Energy Policy*, vol. 184, p. 113862, 2024.